

Assessing the Influence of Asphalt Stabilization on the Deformation Resistance of Reinforced Earth Embankment Model

Saad I. Sarsam^{1*}, Aamal Al-Saidi², Mustafa Falih³

¹Sarsam and Associates Consult Bureau (SACB), Baghdad-Iraq.

²Department of Civil Engineering, College of Engineering, University of Baghdad, Iraq

***Corresponding author**

E-mail Id:-saadisasarsam@coeng.uobaghdad.edu.iq

ABSTRACT

Construction of roadway embankment with Gypseous soil exhibits hazard for the long-term performance. The Gypseous soil is known to exhibit suitable strength after compaction; however, it loses the strength when subjected to environmental issues such as rain and the variation in the water table level. In the present investigation, an attempt has been made to implement Gypseous soil with 84.2 % of gypsum content which was obtained from Tikret region, (180 km north of Baghdad) in the preparation of an embankment model in the laboratory. The Gypseous soil was compacted to 95 % of its maximum pre-determined dry unit weight of (16.4 kN/m^3) in six layers in a metal box with the dimensions of (50 x 50 x 30) cm and each layer is of 5 cm thickness to form a control embankment model, and subjected to vertical stress. Test was carried out using proving ring of 5 kN capacity. The vertical and lateral deformations of the embankment model were monitored until failure. The second embankment model was constructed using an aluminum reinforcing strips spread at five layers of the embankment height. The aluminum reinforcing strips was laid at equal spaces between each of them, which means that each layer was reinforced with four strips at a spacing of 10 cm center to center. The vertical and lateral deformations were also monitored until failure. In the third embankment model, the Gypseous soil was stabilized with M-30 cutback asphalt, then the embankment model was constructed using an aluminum reinforcing strips as in the second model. The fourth embankment model was constructed using the aluminum strips and a stabilized Gypseous soil with cationic emulsion. It was observed that the reinforced and the emulsion stabilized embankment models exhibits lower vertical deformation of (40 and 30) % as compared with the control embankment. On the other hand, the lateral deformation at the third embankment layer declines by (50, 39.2, and 35.7) % when the emulsion, cutback, and earth reinforcements were implemented respectively as compared with the control model. However, the lateral deformation at the fifth layer declines by (68.4, 55.5, and 68.4) % when the emulsion, cutback, and earth reinforcements were implemented respectively as compared with the control model. It was concluded that implementation of cutback and emulsion stabilization in addition to the earth reinforcement can better sustain vertical stresses applied on the embankment surface and present a sustainable solution for the roadway infrastructure.

Keywords:-Asphalt, stabilization, embankment model, reinforced earth, deformation, cutback, emulsion

INTRODUCTION

Large and uneven settlement on the road usually occurs during the service life of the

roadway. Implementation of earth reinforcement and embankment soil

stabilization can reduce these problems. Yujiea et al.,[1] studied the mechanical properties of reinforced soil embankments during its service life. The review utilizes nearby estimated information examination and mathematical reenactment to set up the traffic load model and the killjoy harm model. In light of the examination of the mechanical properties of built up bank under the stacking conditions it was reasoned that when the traffic load recurrence increments from (1 to 4) Hz, the dike settlement is practically steady after 4 Hz. In any case, while the driving stretch is more noteworthy than 4 seconds, the bounce back worth and bounce back time are practically steady. It was revealed that the problems of uneven and large settlements on the road usually happen during the service stage. Reinforced embankments can reduce such problems. Sulovska and Stacho, 2019 verified the design of a reinforced road embankment with a passive facing system. The design was conducted with the aid of the analytical computational model and the numerical modelling, based on the finite element method to obtain the most effective and reliable design. The strain powers for not entirely set in stone through the interior dependability computation. The mathematical demonstrating showed that the bank will implode simultaneously to the two sides and not exclusively to the one of the sides as it was accepted by the scientific methodology. Mante et al., 2021 modeled the proportions of the reinforced embankment and the conventional wall in Plaxis-2D to meet the traffic requirements. Their behavior under various loading circumstances was investigated. It was seen that while the holding wall was reinforced with secures and geogrid under regular stacking conditions, the horizontal and vertical earth pressures were brought down by 3 and 5.5 times, separately. The miss hapenings were more modest under seismic stacking conditions subsequent to

displaying. Sarsam et al.,[2] uncovered that the Gypseous soil is considered as a tricky soil when executed as subgrade layer in the street development. It was recommended to implement asphalt stabilization to retain the required properties of such soil type. Sarsam et al., [3] addressed that plastic geogrid and asphalt stabilization can furnish a suitable solution for enhancing the properties of Gypseous soil which was intended to be used as subgrade soil for road construction. Abdul Ameer et al., [4] \assessed the behavior of earth embankment model prepared from Gypseous soil under static and dynamic loading. Sarsam et al., [5] studied the prospects of stabilizing the collapsible soil with liquid asphalt for modified subgrade construction. An embankment model was constructed in the laboratory and tested under cyclic loading. An endeavor has been made by Rajesh et al., [6] to read up the designing execution for various sorts of subgrade soil built up with geogrid. The California bearing ratio test was conducted in lab and field and the strength of the soil was determined. The influence of geogrid tensile capacity was examined. It was concluded that the influence of plasticity and fines content, and the usage of geogrid in improving the strength are significant. Black-top settled soil and matrix built up soil have been researched by Sarsam and Al Sandok, [7]. For control and black-top balanced out soil, two unique limited component models have been attempted, an axi-symmetric model and a three-layered model. The reinforcement layers were simulated with two deferent models, shell and truss elements. The analysis results were then compared with those of experimental tests. It was concluded that the finite element simulation has given a good agreement with that of experimental tests. The two models have introduced no huge contrast in foreseeing a reasonable twisting. At the point when the support is

addressed by the shell and bracket component, test results have shown a decent understanding among them. Baig and Tiwary, [8] uncovered that supported Earth wall can offer benefits when contrasted and banks and ordinary holding walls for street draws near. The study was carried out using finite element based computer program to find out the deformation of the reinforced retaining wall. Sarsam et al., [9] studied the behavior of reinforced earth model under cyclic loading, the vertical and lateral deformations were detected at different stages of loading cycles using LVDT. It was uncovered that the reduction and emulsion balanced out soil model show improvement in load conveying limit by nine and twenty folds. However, a reduction of (23 and 38.5) % in vertical displacement under sustained load of 436 and 950 repetitions respectively was observed. The analytical expressions of the lateral deformation of ground under the infinite long line load, was derived by Liu et al., [10] 2018. The influence of the width of embankment on the lateral deformation was analyzed. The result shows that the maximum deformation is at a depth below the ground surface. However, the Poisson's ratio has a significant influence on the lateral deformation of ground. The higher the Poisson ratio is, the more the horizontal displacement of the soil will have. Zhang et al., [11] determined the dispersion of the heap on the fortifications and association strength expected for each layer of the Geosynthetic built up soil. All of the possible failure surfaces were considered with the aid of the top-down procedure involved for the seismic analyses. The distributions of load were used to determine the required connection strength and to approximately assess the facing lateral deformation. It was revealed that the maximum required tensile resistance is identical. Nonetheless, short support brings about more prominent

elastic protections in the lower and mid layers. The misshaping of the bank was concentrated by Lv et al., [12] through the dike model test, and the settlement estimation technique was proposed. It was recognized that the horizontal twisting of the dike was straightforwardly corresponding to the upward disfigurement, in any case, sliding happens under a definitive burden, and the bearing limit is lost. It was concluded that the deformation is calculated by the formula, and the difference between the settlement and the model test data is 6.2%, which proves the feasibility and accuracy of the calculation method. Liu et al., [15] revealed that excessive deformation of the asphalt mixture is related to the decrease of the material's stability due to the increase of unfavorable stress state, high shear stress, and low confining pressure, which can lead to significant nonlinear visco-plastic behavior. It was accounted for that the complete misshapening of the black-top combination through stacking and rest cycle can be isolated into three sections, being flexible, visco-versatile, and visco-plastic strain. The point of the current work is to survey the impact of black-top adjustment on the twisting opposition of supported earth dike model. Laboratory models will be prepared for control, reinforced, cutback stabilized, and emulsion stabilized Gypseous soil. The models will be tested under static load and the vertical and lateral deformations will be monitored and compared.

MATERIALS PROPERTIES AND TESTING METHODS

Gypseous soil

The implemented Gypseous soil was obtained from Tikret region, (180 km north of Baghdad) at middle north part of Iraq. The top soil of one meter depth was removed using a shovel, then the soil was taken from a depth of (1.0 to 1.75) m below the lower level of the top soil. The

soil sample was pulverized using a plastic hammer, then sieved through sieve No. 4. The passing portion of the soil was implemented for the detailed testing program. The soil sample was subjected to testing for physical properties according to ASTM, 2015 specification requirements.

Table 1 demonstrates the chemical composition of the soil. However, Table 2 exhibits the important physical properties. Figure 1 shows the grain size distribution of the soil.

Table 1:-Chemical composition of the soil

Chemical composition	Results
Total Soluble Salts (T.S.S.)	76.40%
Total (CO ₃)	0.51%
pH value	7.70
Gypsum Content	84.28%

Table 2:-Physical properties of the Gypseous soil

Physical characteristics	Result
Specific Gravity	$G_s = 2.2$
Liquid Limit	L.L. = 19.65
Plasticity Index	P.I. = Non-Plastic Soil
Maximum Dry Unit Weight (Standard Compaction)	$\gamma_d \text{ max} = 17.1 \text{ kN/m}^3$
Optimum Moisture Content (Standard Compaction)	$\omega = 12.3\%$
Maximum Dry Unit Weight (Modified Compaction)	$\gamma_d \text{ max} = 20.9 \text{ kN/m}^3$
Optimum Moisture Content (Modified Compaction)	$\omega = 7.3\%$
Coefficient of Uniformity	$C_u = 2.82$
Coefficient of Curvature	$C_c = 1.14$
Unified Classification System	SM
Direct shear strength and Angle of internal friction	7 KPa, 32°

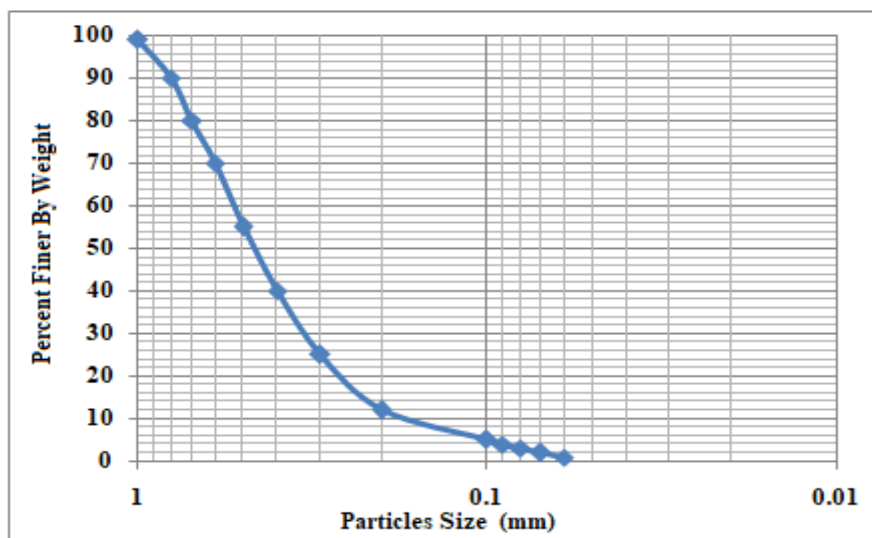


Fig.1:-Grain size distribution of the soil

Cutback Asphalt

Medium curing Cutback asphalt of MC-300 was obtained from Dourah oil

refinery-Baghdad. The important physical properties of the cutback asphalt were verified and listed in Table 3.

Table 3:-Properties of Cutback Asphalt

Property	Test Results
Kinematic viscosity at 60°C (c. stoke)	0.33
Specific gravity	45
Distillation	
Distillate % vol. of total distillate to 360°C.	
To 225°C	25 max
To 260°C	40 – 70
To 315°C	75 – 93
Residue from distillation to 360°C %vol. By difference	50 min.
Tests on residue from distillation	
Penetration at 25°C (100gm, 5 sec.)	120 – 300
Ductility at 25°C (5cm/min)	100 min.
Solubility in carbon tetrachloride CCl ₄ % wt.min	99.5 min.

Cationic emulsified asphalt

Cationic emulsified asphalt was obtained from Dourah oil refinery; the physical properties of the emulsion are listed in Table 4.

Table 4:-Properties of cationic Emulsion

Property	Test Results
Particles Charge	+ positive
Kinematic Viscosity (c. stoke)	45
Cement Mixing (%)	1.2
Settling Time (hr.)	19
Coating ability & water resistance	Good
Coating dry & wet aggregate	Fair

Reinforcing strips

Smooth aluminum reinforcing strips of one mm thickness, 500 mm length, and 20 mm width were prepared and implemented as earth reinforcement for the embankment model.

Preparation for deformation test of the control embankment model

The embankment model box of (500 x 500 x30) mm was prepared; the soil was mixed with the optimum water content, then

compacted in six layers of 50 mm thickness to the target maximum dry unit weight of (16.4 kN/m³). Test was carried out using a proving ring of 5 kN capacity. The vertical dial gage was installed to capture the deformations of the embankment model. However, two dial gages were assembled at the 3rd and 5th layer surface of the embankment model to capture the lateral deformation of the soil model. Figure 2. Present the test setup. More details on the preparation of the

embankment model could be found in Sarsam et al.,[17].

Preparation for deformation test of the reinforced embankment model

The embankment model box of (500 x 500 x30) mm was prepared; the soil was mixed with the optimum water content, then compacted in six layers of 50 mm thickness to the target maximum dry unit weight of (16.4 kN/m³). The aluminum strips of one mm thickness, 500 mm length, and 20 mm width were installed on the surface of each compacted soil layer.

The aluminum reinforcing strips was laid at equal spaces between each of them, which means that each layer was reinforced with four strips at a spacing of 100 mm center to center. Test was carried out using a proving ring of 5 kN capacity. The vertical dial gage was installed to capture the deformations of the embankment model. However, two dial gages were assembled at the 3rd and 5th layer surface of the embankment model to capture the lateral deformation of the soil model. Figure 2. Present the test setup.



Fig.2:-Control and Stabilized soil embankment models

Preparation for deformation test of the reinforced and stabilized embankment model

The embankment model box of (500 x 500 x30) mm was prepared; the soil was mixed with the optimum water content, then the optimum requirement of cutback or emulsion was added, thoroughly mixed, then compacted in six layers of 50 mm thickness to the target maximum dry unit weight. Subtleties of getting the ideal fastener content could be alluded to Sarsam et al., 2014. The aluminum strips of one mm thickness, 500 mm length, and 20 mm width were installed on the surface of each compacted soil layer. The aluminum reinforcing strips was laid at

equal spaces between each of them, which means that each layer was reinforced with four strips at a spacing of 100 mm center to center. Test was carried out using a proving ring of 5 kN capacity. The vertical dial gage was installed to capture the deformations of the embankment model. However, two dial gages were assembled at the 3rd and 5th layer surface of the embankment model to capture the lateral deformation of the soil model. The Models were cured for seven days in the laboratory environment so that the volatiles of the liquid asphalt binder can evaporate.

RESULTS AND DISCUSSIONS

Influence of applied pressure on vertical deformation

Figure 3 demonstrates the influence of the applied pressure on the vertical deformation of the tested embankment models. It can be observed from Figure 3-left that the control soil embankment model (un-stabilized, un-reinforced) exhibit failure at the early stages of loading (after 0.5 MPa) of applied pressure and shows a vertical deformation of 0.26 mm. However, when the aluminum reinforcing strips are incorporated in the soil embankment model, higher load sustainability of 2.4 MPa could be noticed accompanied with lower vertical deformation of 0.18 mm. On the other hand, when the liquid asphalt was introduced, high load sustainability of (0.2, and 1.8) MPa could be detected for emulsion and cutback treated soil model respectively. However, the emulsion

stabilized soil exhibit no significant variation in the rate of deformation as compared with the reinforced soil, while the cutback stabilized soil exhibit significant variation in the rate of deformation as compared with the reinforced or emulsion stabilized soil model. This may be attributed to the fact that the volatiles in the cutback require more time to evaporate so that the viscosity of the asphalt residue and the stiffness of the stabilized soil increase. Such behavior is further supported in Figure 3-right, where the scatter of the relationship between the vertical deformation of the control soil model and the cutback stabilized soil model is mostly above the 45° line. Table 5 demonstrates the mathematical models obtained from Figure 3-right, the polynomial equation models exhibit high coefficient of determination.

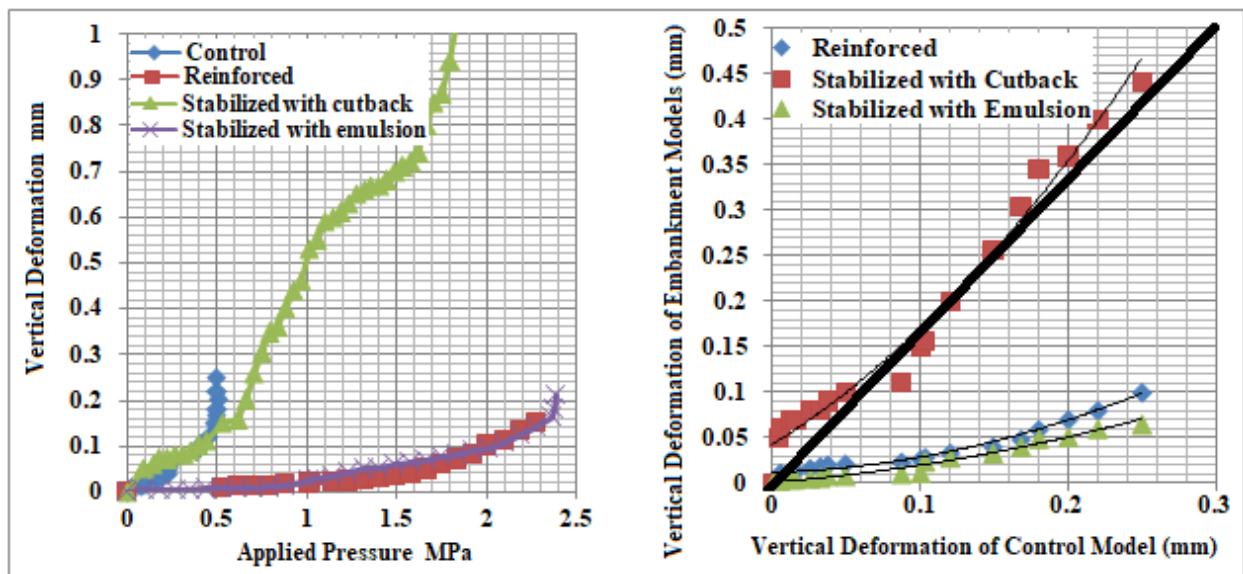


Fig.3:-Influence of applied pressure on vertical deformation

Table 5:-Modeling the influence of applied pressure on vertical deformation

Vertical Deformation (mm)	Mathematical Model	R ²
Reinforced Earth	$Y = 2.755 x^2 + 1.007 x + 0.041$	0.978
Reinforced and Stabilized with Cutback	$Y = 1.21 x^2 + 0.046 x + 0.01$	0.979
Reinforced and Stabilized with Emulsion	$Y = 0.592 x^2 + 0.126 x + 0.001$	0.974

Influence of applied pressure on lateral deformation

Figure 4 exhibit the influence of applied pressure on lateral deformation of the embankment models. Sharp trend of increase in the lateral deformation of the control soil model accompanied with early failure of 2.8 mm deformation after 0.5 MPa load could be detected as the loading proceeds. However, when the reinforcements are introduced, the lateral deformation at failure declines by (36, and 67) % at the third and fifth layers respectively as compared with the control

soil. When the liquid asphalt was mixed with the soil of the reinforced embankment model, the emulsion treated soil exhibit lower lateral deformation than the cutback treated soil. The lateral deformation of the emulsion treated soil at failure declines by (50, and 66) % at the third and fifth layers respectively as compared with the control soil. On the other hand, the lateral deformation of the cutback treated soil at failure declines by (36.7, and 50) % at the third and fifth layers respectively as compared with the control soil.

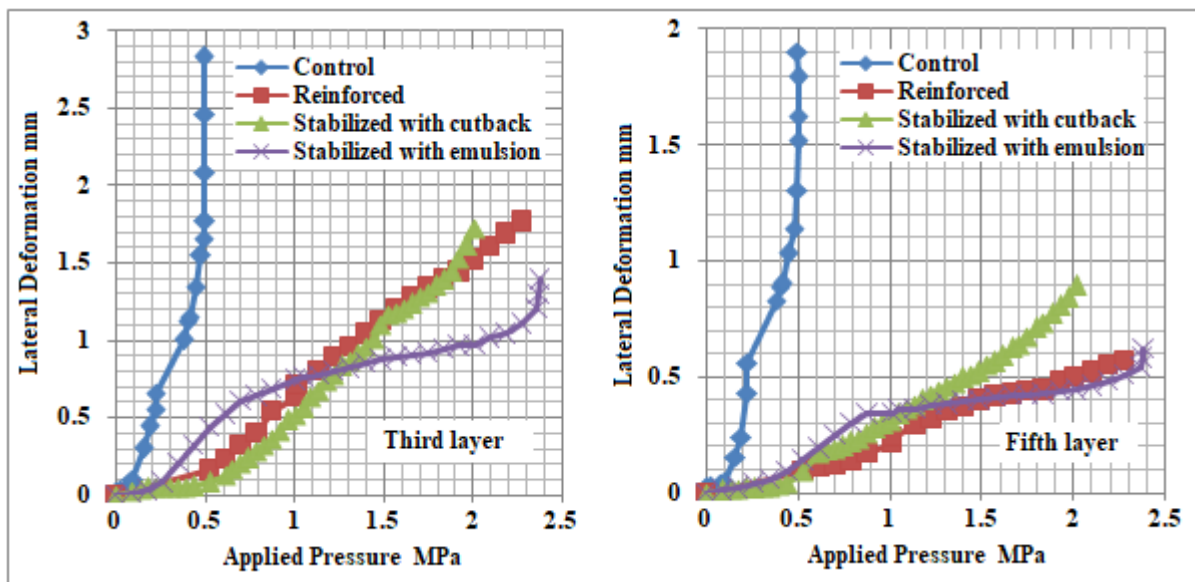


Fig 4. Influence of applied pressure on lateral deformation

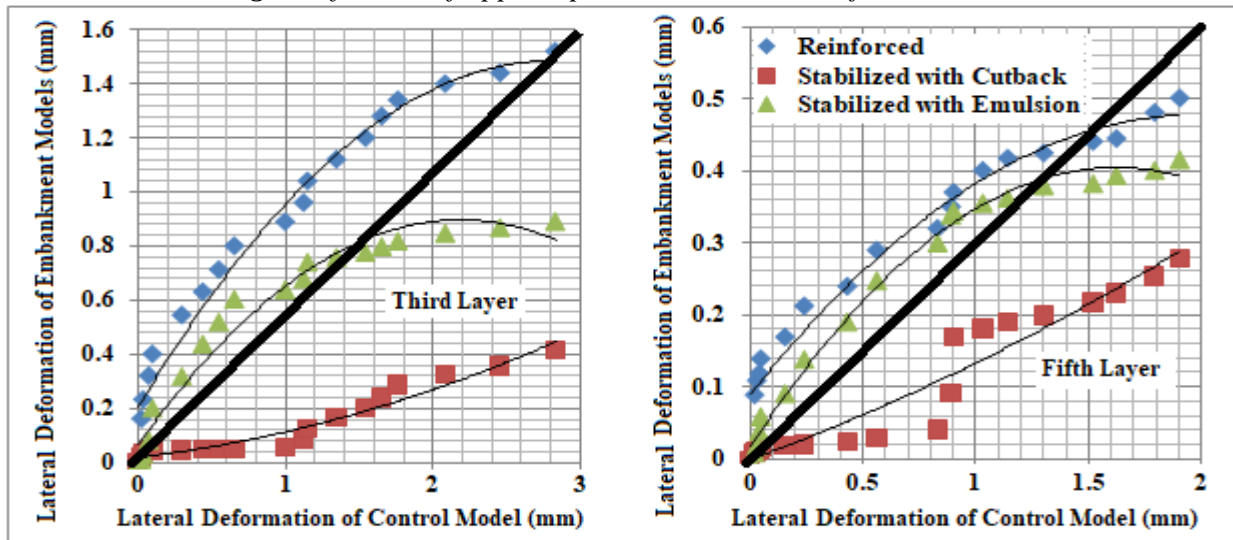


Fig.5:-Modeling the influence of applied pressure on lateral deformation

Figure 5 demonstrates the modeling of the influence of applied pressure on lateral deformation for both third and fifth layers of the soil embankment models. It can be noticed that the scatter of the lateral deformation of the emulsion stabilized and reinforced soil models is mostly above the 45° line, while it is below

the 45° line for cutback stabilized soil model regardless of the location of the monitored layer. Tables 6 and 7 exhibits the mathematical models obtained. The polynomial conditions show high coefficients of assurance no matter what the stabilizer type or the layer area.

Table 6:-Mathematical models for 3rd layer

Lateral Deformation at Third Layer (mm)	Mathematical Model	Coefficient of Determination R ²
Reinforced Earth	$Y = -0.164x^2 + 0.919x + 0.201$	0.977
Reinforced and Stabilized with Cutback	$Y = -0.174x^2 + 0.762x + 0.063$	0.966
Reinforced and Stabilized with Emulsion	$Y = 0.031x^2 + 0.064x + 0.015$	0.950

Table 7:-Mathematical models for 5th layer

Lateral Deformation at fifth Layer (mm)	Mathematical Model	Coefficient of Determination R ²
Reinforced Earth	$Y = -0.098x^2 + 0.391x + 0.089$	0.966
Reinforced and Stabilized with Cutback	$Y = -0.147x^2 + 0.477x + 0.017$	0.992
Reinforced and Stabilized with Emulsion	$Y = 0.019x^2 + 0.113x$	0.922

Influence of applied pressure on Poisson ratio

Poisson's ratio is a measure of the stability which balances the deformation of a material in directions perpendicular to the specific direction of loading. It is how much cross-over prolongation separated by how much pivotal pressure. Figure 6

exhibit the fluctuation of Poisson ratio throughout the applied pressure for the tested soil models. Similar trend of variation in the Poisson ratio could be observed among the monitored layer. However, significant variation in the Poisson ratio is observed for control soil model through the loading process.

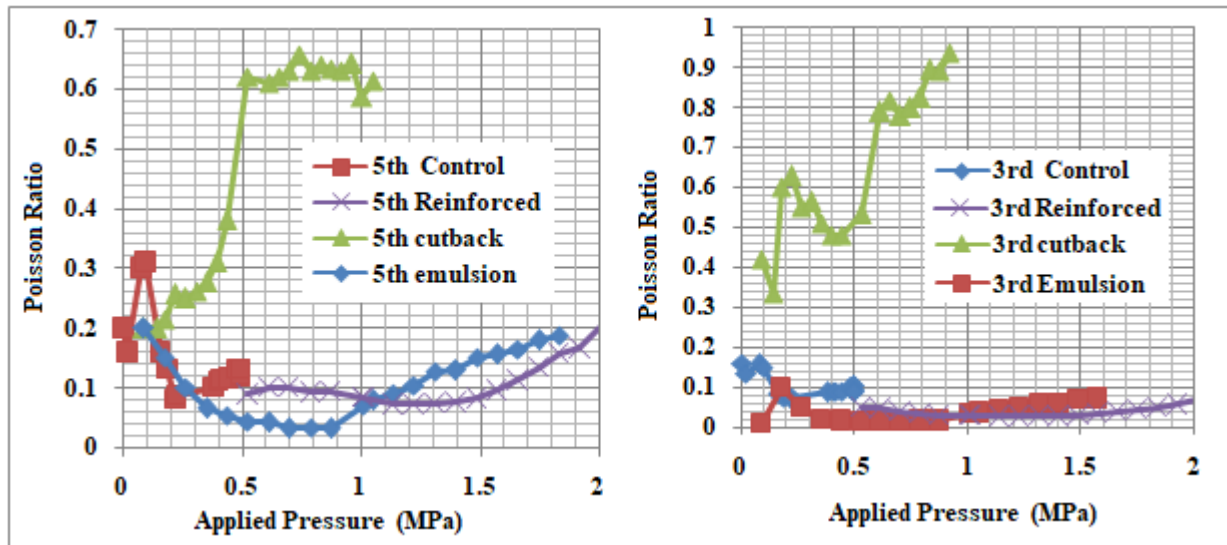


Fig.6:-Fluctuation of Poisson ratio

The Poisson ratio fluctuates from (0.08 to 0.3) under loading at the upper layer (5th layer) while it fluctuates from (0.1 to 0.18) under loading at the lower layer (3rd layer). This may be related to the decline in pressure bulb at the lower layer. When the aluminum reinforcing strips were introduced, the fluctuation in the Poisson ratio was minimal through the loading process, the reinforcement of the soil was capable to control the tensile stresses applied which is more pronounced at the third layer. On the other hand, when the reinforced soil was treated with cationic emulsion, the Poisson ratio fluctuates from (0.02 to 0.2) under loading at the upper layer (5th layer) while the fluctuation of Poisson ratio was not significant at the lower layer (3rd layer). When the reinforced soil was stabilized with cutback asphalt, significant variation in the Poisson ratio could be detected regardless of the monitored layer location. The Poisson ratio fluctuates from (0.2 to 0.65) under loading at the upper layer (5th layer) while it fluctuates from (0.3 to 0.95) under loading at the lower layer (3rd layer). Failure of the stabilized soil models occurred at early stage of loading as compared with that of the reinforced soil model regardless of the layer location. It

tends to be seen that adjustment of the built up soil with reduction black-top shows higher Poisson proportion as contrasted and that of adjustment of supported soil with cationic emulsion. More stable embankment is created when reinforcement and emulsion are implemented as indicated by limited fluctuations in the Poisson ratio. Similar behavior was reported by Lv et al., 2021.

CONCLUSIONS

The following remarks may be addressed based on the testing program and limitations of materials.

- 1- Higher load sustainability of (2.4, 0.2, and 1.8) MPa could be noticed for the reinforced, emulsion and cutback treated soil respectively as compared with the control embankment model.
- 2- The lateral deformation at failure declines by (36, and 67) %, (50, and 66) %, and (36.7, and 50) % at the third and fifth layers respectively as compared with the control soil when the reinforcement, emulsion, and cutback were implemented.
- 3- Lower vertical deformation of 0.18 mm could be detected when reinforcements were introduced as compared with the control model. However, emulsion stabilized soil exhibit no significant

variation in the rate of deformation, while the cutback stabilized soil exhibit significant variation in the rate of deformation as compared with the reinforced or emulsion stabilized soil model.

4- The Poisson ratio fluctuates from (0.08 to 0.3) under loading at the upper layer (5th layer) while it fluctuates from (0.1 to 0.18) under loading at the lower layer (3rd layer) for control model. The fluctuation in the Poisson ratio was minimal through the loading process when the reinforcements were introduced.

5- The Poisson ratio fluctuates from (0.02 to 0.2) under loading at the upper layer (5th layer) while the fluctuation of Poisson ratio was not significant at the lower layer (3rd layer) for emulsion treated soil.

6- When the reinforced soil was stabilized with cutback asphalt, the Poisson ratio fluctuates from (0.2 to 0.65) under loading at the upper layer (5th layer) while it fluctuates from (0.3 to 0.95) under loading at the lower layer (3rd layer).

7- More stable embankment is created when reinforcement and emulsion are implemented as indicated by limited fluctuations in the Poisson ratio.

REFERENCES

1. Yujie H., Bo W., Liang H., Weili H., Jiahua Z., Junjie W. Mechanical properties of re-packed reinforced Earth embankment during service stage. *Journal of Asian Architecture and Building Engineering*. Building structures and materials. 21(4):1520-1531.
<https://doi.org/10.1080/13467581.2021.1930010>.
2. Sarsam S., AL-Saidi A., AL-Khayat B. Implementation of Gypseous soil-asphalt stabilization technique for base course construction. *Journal of Engineering*, Vol. 17 No.5, December 2011. (P 1066- 1076).
3. Sarsam S.; AL-Saidi A. and Mukhle O. Behavior of Reinforced Gypseous Soil Embankment Model under Cyclic Loading. *Journal of Engineering*, Volume 19 No.7, July 2013.
4. Abdul Ameer H.; Sarsam S.; Ahmed M. Studying the Behavior of Asphalt Stabilized Gypseous Soil for Earth Embankment Model. *Journal of Engineering*, Number 5 Volume 20 May – 2014. (P 25-43).
5. Sarsam S., Al Saidi A., Al Taie A. Assessment of shear and compressibility properties of asphalt stabilized collapsible soil. *Applied Research Journal* Vol.2, Issue, 12, pp.481-487, December 2016.
6. Rajesh U., Sajja S., Chakravarthi V. Studies on Engineering Performance of Geogrid Reinforced Soft Subgrade. Elsevier, *Transportation Research Procedia*. Volume 17, 2016, Pages 164-173.
<https://doi.org/10.1016/j.trpro.2016.11.072>.
7. Sarsam S., AL Sandok A. Modeling the deformation of stabilized and reinforced subgrade soil. *Journal of Modern Technology & Engineering*. Jomard publishing. Vol.3, No.1, 2018, pp.143-154.
8. Baig A., Tiwary A. Behavior & stability analysis of geogrid reinforced earth wall: a case study in vizianagaram (A. P.). *International Journal of Civil Engineering and Technology (IJCET)*. Volume 10, Issue 04, April 2019, pp. 1987- 2000, Article ID: IJCET_10_04_198 Available online at <http://www.iaeme.com/ijmet/issues.asp?JType=IJCET&VType=10&IType=4>.
9. Sarsam S., Alsaidi A., Alzobaie O. Impact of Asphalt Stabilization on Deformation Behavior of Reinforced Soil Embankment Model under Cyclic

- Loading. Journal of Engineering Geology and Hydrogeology JEGH 2014, 2(4):46-53. Sciknow publication Ltd. USA.
10. Liu G., Li Y., Cao Y. Calculation and analysis of lateral deformation of ground under embankment load. Yantu Lixue/Rock and Soil Mechanics 39(12):4517-4526 and 4536. December 2018. DOI: 10.16285/j.rsm.2017.1045.
 11. Zhang, F., Zhu, Y., Chen, Y. Yang S. 2021. Seismic effects on reinforcement load and lateral deformation of Geosynthetic-reinforced soil walls. Front. Structural and Civil. Engineering.. 15, 1001–1015 (2021). <https://doi.org/10.1007/s11709-021-0734-8>.
 12. Sulovska M. Stacho J. design of a road embankment reinforced using a geogrid. 19th SGEM International Multidisciplinary Scientific Geo-Conference EXPO Proceedings. June 2019. <https://www.researchgate.net/publication/334734164>.
 13. Mante V., Mohammed F., Gorla K. Seismic response of mechanically stabilized earth wall for widened embankment. International Research Journal of Engineering and Technology (IRJET) Volume: 08 Issue: 12 | Dec 2021 www.irjet.net.
 14. Lv Gh., Cui W. & Wang Sj. Model Test and Theoretical Analysis of New and Old Embankments.
 15. Differential Settlement Considering Lateral Deformation. Springer Geotech Geol Eng 39, P. 5743–5751, 2021. <https://doi.org/10.1007/s10706-021-01862-4>.
 16. Liu X., Zhang M., Liu W. The relationship between Poisson's ratio index and deformation behavior of asphalt mixtures tested through an optical fiber bragg grating strain sensor. Materials 15(5):1882. March 2022. DOI: 10.3390/ma15051882.
 17. ASTM, 2015. Road and Paving Materials, Annual Book of ASTM Standards, Volume 04.03, American Society for Testing and Materials,
 18. Sarsam S., Al-Saeidy A., Falihi M. 2014. Assessing Pullout Resistance of Earth Reinforced Embankment Model. Journal of Engineering Geology, and Hydrogeology. JEGH, Sciknow Publications Ltd., 2(1):9-14 DOI: 10.12966/jegh.02.02.2014.